From Reflow to Fatigue: A Continuum Damage Mechanics Framework Incorporating Individualized As-Reflowed Solder Geometry

Henan Mao, Junyan He, Linqi Zhuang and Adarsh Chaurasia
Synopsys, Inc
675 Almanor Ave
Sunnyvale, CA 94085 US
Email: linqiz@synopsys.com

Abstract

In this paper, we propose a Multiphysics simulation framework that couples the complex solder reflow process directly with continuum damage mechanics (CDM)-based fatigue prediction under thermal cycling. The solder reflow process was first simulated in Ansys LS-DYNA using the Incompressible Smoothed Particle Galerkin (ISPG) method, which accurately captures molten solder flow, surface-tension-driven wetting behavior, and solidification. An in-house morphing algorithm mapped a high-quality, all-hexahedral template mesh onto each as-reflowed solder geometry for solder fatigue analysis. A CDM-based analysis was conducted to simulate the solder damage initiation and propagation under thermal cycling. To improve computational efficiency, a cycle-jump algorithm was also adopted, skipping large percentages of intermediate thermal cycles based on predefined criteria. Results demonstrate that the proposed workflow captures experimentally observed solder failure processes well, clearly validating the critical influence of manufacturing-induced geometric variation on predicted fatigue life.

Key words

Continuum Damage Mechanics, Finite Element, Multiphysics, Solder Reflow, Solder Fatigue

I. Introduction

In modern electronics, solder fatigue is a major cause of system failure. Engineers commonly use empirical, strain-based, or energy-based models to estimate fatigue life [1]. Although these methods are practical for conventional solder fatigue workflows because they require only a few simulated cycles to obtain stabilized quantities for life prediction, they do not capture the evolution of internal damage. This limitation is important in applications such as digital twins, where real-time tracking of material degradation is needed to predict remaining useful life. In addition, standard numerical analyses often assume idealized, uniform solder geometries, even though manufacturing variations can produce irregular wetting angles, asymmetric fillets, and other shape differences. Previous work [2] has shown that solder geometry significantly affects fatigue behavior. Therefore, accurate geometric representation is essential for reliable prediction. To address this limitation, in this paper, we propose a Multiphysics framework that links solder reflow simulation with CDM-based fatigue modeling using the exact solder geometries predicted by the reflow analysis.

II. Methods

A. Solder Reflow Simulation

Many semiconductor packaging processes involve free-surface flow, wetting, surface tension, and contact-angle behavior [3]–[6]. In BGA solder reflow, molten solder evolves under the combined effects of capillary forces, gravity, surface tension, and wall adhesion, eventually forming the final solder-joint geometry after solidification. Similarly, in adhesive dispensing, viscous polymer materials are extruded, spread, stretched, and separated to form droplets or beads. In thermocompression bonding, local material flow and interface formation occur under coupled thermal and mechanical loading. These process-dependent material-flow behaviors directly influence electrical connectivity, bond quality, defect formation, and long-term package reliability [3], [7], [8].

Numerical modeling of these processes is challenging due to large fluid deformation, free-surface evolution, coalescence, separation, and interactions with complex solid boundaries. Analytical approaches are useful for simplified equilibrium estimates but are generally inadequate for transient simulations of realistic package geometries. Although Eulerian CFD methods can model free-surface flow, interface reconstruction, contact-line treatment, and coupling

with moving or deformable structures can be difficult in large-scale packaging applications [3], [4]. Lagrangian particle methods offer an attractive alternative by naturally tracking the material interface through particle motion, thereby avoiding explicit interface reconstruction.

The Incompressible Smoothed Particle Galerkin (ISPG) method implemented in LS-DYNA provides a stabilized Lagrangian particle-Galerkin formulation for incompressible free-surface flow [3], [4]. ISPG uses momentum-consistent velocity smoothing and a pressure-correction scheme to improve numerical stability while retaining the natural interface-tracking capability of particle methods. The method also includes surface-tension and wall-adhesion/contact-angle treatments, making it suitable for modeling solder reflow processes involving wetting-driven shape evolution.

Fig. 1 shows a representative BGA solder reflow simulation performed in LS-DYNA using the ISPG method in this study. During reflow, the molten solder balls deform and redistribute under surface tension and wetting forces until they approach their equilibrium joint shapes. In the present study, to demonstrate the proposed workflow, one of the critical regions that contains 4 solders were extracted from the full board model and used for later solder fatigue analysis.

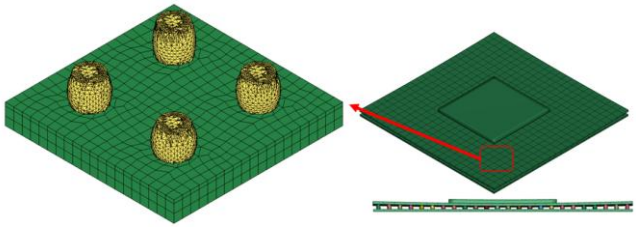


FIGURE 1: DEFORMED SOLDER BALL SHAPES AFTER REFLOW

B. As-reflowed solder geometry remeshing

After the solder reflow simulation, the as-reflowed solder-joint geometry is exported from LS-DYNA by generating a triangulated surface from the final particle positions at the solder solidification temperature (Fig. 1). This tetrahedral mesh is for visualization only and usually does not have high element quality required for nonlinear thermal cycling analyses with complex material models. As such, an in-house approach based on mesh morphing is developed to generate high-quality all-hexahedral mesh for the as-reflowed solder shape. First, an all-hexahedral mesh template for a solder joint is generated from an idealized truncated sphere shape, see Fig. 2:

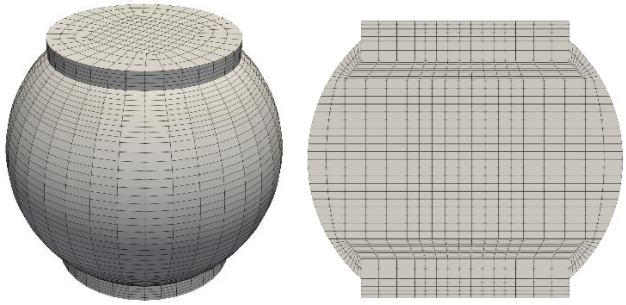


FIGURE 2: TYPICAL TEMPLATE MESH FOR AN IDEALIZED SOLDER SHAPE

Note that the user has the option to change the mesh sizes on the template mesh to achieve different mesh density on the as-reflowed solder shape. Since the LS-DYNA exported mesh does not always contain valid element connectivity and might have intersecting edges/elements, direct morphing to the target shape is not adopted here. Instead, we sample the cross section of the as-reflowed solder shape at different Z heights. The cross sections are in the form of 2D point clouds on the exterior surface of the as-reflowed solder shape. To minimize the effect of surface artifacts in the initial tetrahedral mesh, least-squared curve fitting is employed to fit an ellipse to the 2D points. The major and minor axes, center and tilt of the ellipse can be identified from the curve fit, allowing us to capture the approximate shape of the cross section while filtering out any potential noise. Then, mesh morphing is carried out to morph the circular cross section of the template mesh at each Z height to the fitted elliptical profile at the corresponding height. This leads to an all-hexahedral mesh for the as-reflowed solder shape that is otherwise difficult to generate directly, see Fig. 3. It should be noted that all 4 solders studied here have different shapes after reflow process.

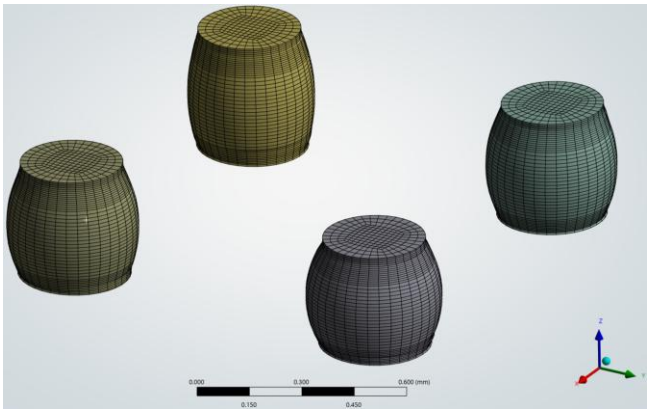


FIGURE 3: MORPHED ALL-HEXAHEDRAL MESH FOR THE AS-REFLOWED SOLDER SHAPES

For simplicity, in this work, the mesh interfaces between the solder and the PCB and copper pads are not conformal, and bonded contact is used to connect the parts together. While this is not the optimal solution, future work will investigate

generation of fully conformal meshes for the as-reflowed BGA assembly.

C. Solder Fatigue Analysis

During thermal cycling, solders usually go through excessive nonlinear deformation, which results in potential damage. To account for such non-brittle typed damage, in this paper, a regularized gradient-enhanced damage approach developed by B Yin, Z Imadeddin, Z Dong, A Raasheduddin, L Guoyu and K Michael [9] was adopted. The internal damage variable equation was initially proposed by C Sommitsch, S Rainer, W Thomas, G Burkhard and W Volker in [10]. The key components of the proposed damage model are as follows: model, the evolution of the damage is governed by an internal quantity η:

$$\eta = \int_0^{t_{n+1}} \dot{\eta} dt \tag{1}$$

Where

$$\dot{\eta} = \left(\frac{\sigma_{eq}}{A_0}\right)^{M_0} \left(\frac{\dot{P}}{\dot{p}_0}\right)^{N_0} \dot{p}_0 \tag{2}$$

σ_{eq} and $\dot{P}$ are von-Mises equivalent stress, and inelastic Mise's strain-rate that considers both plasticity and creep of the solder, respectively. A_0, $\dot{p}_0$, M_0 and N_0 are constant material dependent parameters. To avoid numerical singularities, a non-local representation of the internal variable η is represented as

$$\bar{\eta} - c\nabla^2\bar{\eta} = \eta \tag{3}$$

c is the internal length effect parameter. An exponential softening function is then defined as

$$d = 1 - \exp\left(-Z\langle\bar{\eta} - \eta_{cr}\rangle_+\right) \tag{4}$$

Damage starts when $\bar{\eta}$ reaches critical threshold η_{cr}. The coefficient Z determines the rate of softening. The operator $\langle * \rangle_+ = \frac{* + |*|}{2}$, which is known as the MACAULEY bracket.

Simulating cyclic loading could be computationally expensive. To speed up the analysis, a cycle-jump numerical technique that approximates long-term system response using an evolution function for selected variables was implemented in this paper. Rather than simulating every cycle, the solver extrapolates and skips intermediate cycles.

In the present study, the global control variable (Pn shown in Fig. 4) was chosen as equivalent plastic strain, a variable-based jump criterion was adopted

$$\Delta t^M_{y,jump} = q_y \Delta t_{cycle} avg\left(\frac{|y_2|}{|y_1 - y_2|}, \frac{|y_3|}{|y_2 - y_3|}\right) \tag{5}$$

Where q_y is a user defined constant that would determine the size of the jump. In this study, $q_y = 5$. A jump occurs when $\Delta t^M_{y,jump}$ is greater than the cycle time. If a jump occurs, all variables needed for a finite element analysis (such as stress, strain, state variables, and degrees of freedom) are extrapolated based on (6). The extrapolated state is imposed as the new state at time t0 after the jump.

$$y(t_1 + \Delta t_{jump}) = y(t_1) + \frac{1}{2}(s_{12} + s_p)\Delta t_{jump} \tag{6}$$

Where

$$s_p = s_{12} + \frac{s_{12} - s_{23}}{\Delta t_{cycle}} \Delta t^M_{y,jump} \tag{7}$$

s_{12} and s_p are slopes for each period, as shown in Fig. 4.

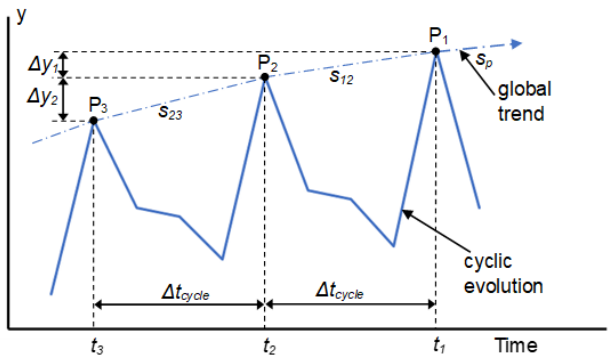


FIGURE 4: TYPICAL STRUCTURAL RESPONSES UNDER CYCLIC LOADING

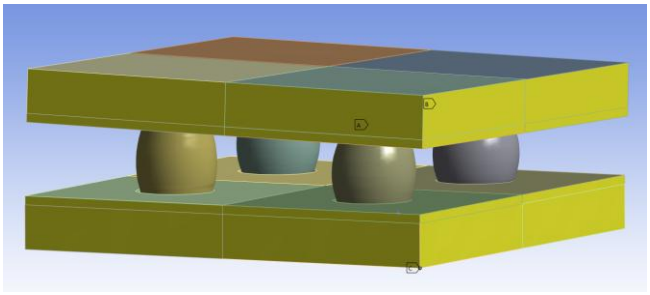


FIGURE 5: ILLUSTRATION OF BOUNDARY CONDITIONS

Once the as reflowed geometry has been remeshed, as discussed in the previous section. The meshed model was imported into Ansys Mechanical to set up the solder fatigue analysis. The boundary conditions for the model are displayed in Fig. 5. For the highlighted faces, the translational degree of freedom (DoF) normal to the corresponding face is constrained, an additional through thickness translational DoF is constrained at the bottom corner node (point C in Fig. 5) to avoid rigid body motion.

The whole model goes through the same temperature cycle as shown in Fig. 6.

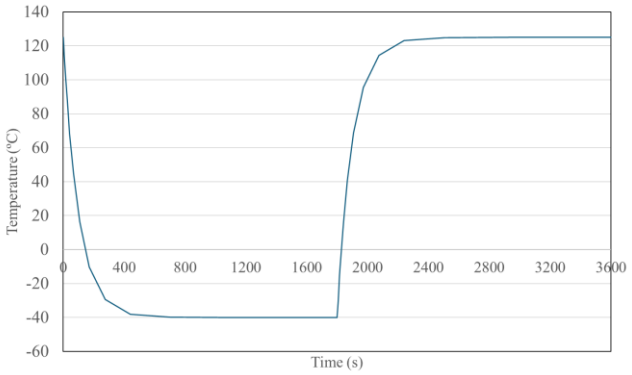


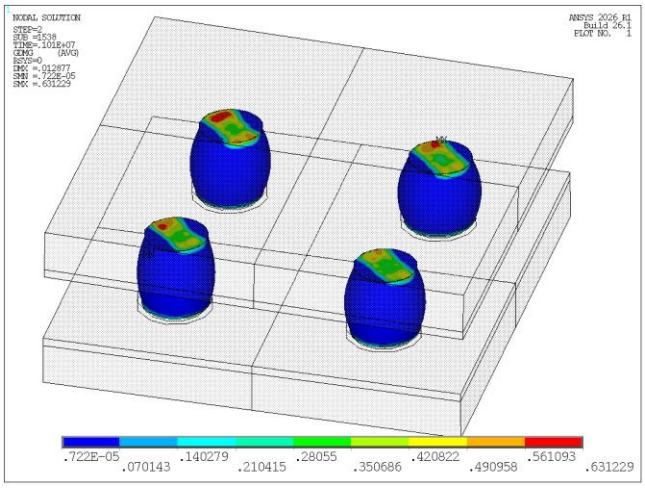
FIGURE 6: TEMPERATURE CYCLE

The corresponding parameters for the damage model in (2) are listed in Table 1. It should be noted that the parameters were selected to ensure meaningful damage propagation within the simulated cycles. As mentioned in the previous section, those parameters are material dependent, which should be calibrated.

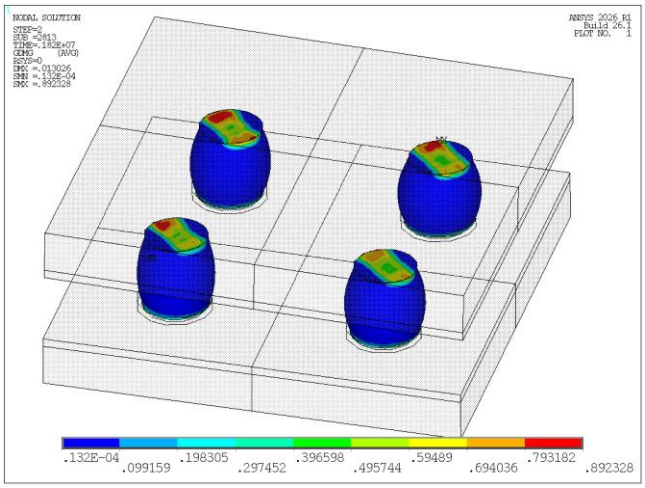
TABLE 1: GENERALIZED DAMAGE MODEL PARAMETERS

A_0 (Pa)	$3.306e^{7}$
M_0	0.7
$\dot{p}_0$ (1/s)	0.6
N_0	0.8
c (mm^2)	$1.44e^{-4}$
Z	0.06
η_{cr}	0

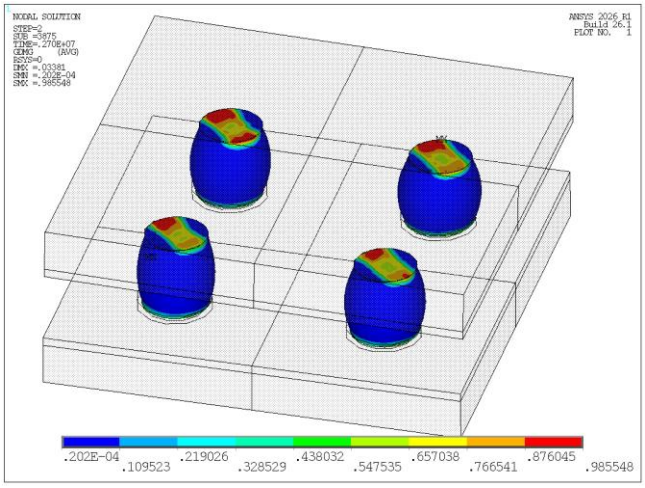
In this study, a total of 1000 thermal cycles were analyzed. 77% of the 1000 cycles were skipped with cycle-jump implemented, which greatly reduces the total compute time. In total, the simulation was solved in 13.7hrs with 32 cores. Further speed up could be achieved with more cores. The simulated damage index at top side of the solders at different cycles is shown in Fig. 7. The view angle is consistent with one shown in Fig. 3. As demonstrated in Fig. 7, higher damage indexes are located near the interface between the solder and copper pad interface at top two solders. The damage index then increases with increasing cycles, and high damage areas propagate from outside to inside. Similar pattern could be found at the bottom of the solders, as shown in Fig. 8.



(a)



(b)



(c)

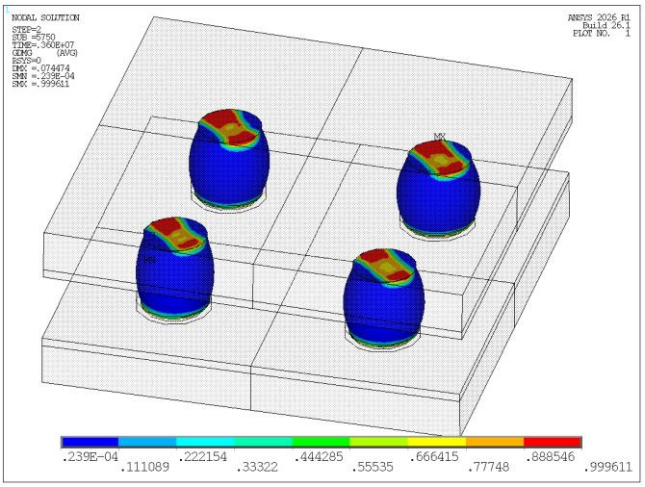


FIGURE 7: DAMAGE AFTER (A) 280.5 CYCLES, (B) 500 CYCLES, (C) 750 CYCLES, AND (D) 1000 CYCLES

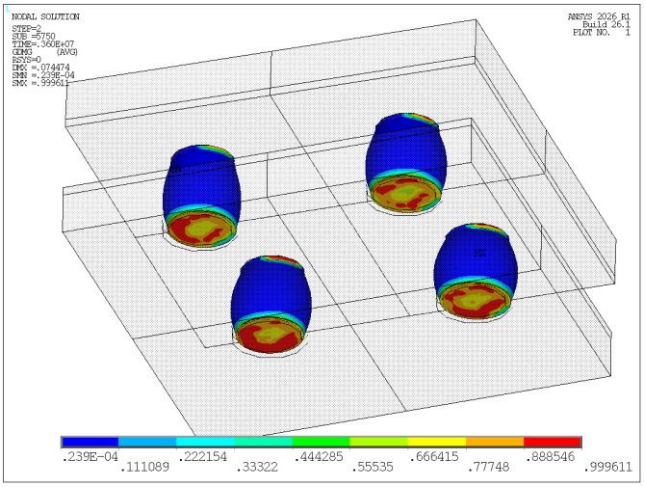
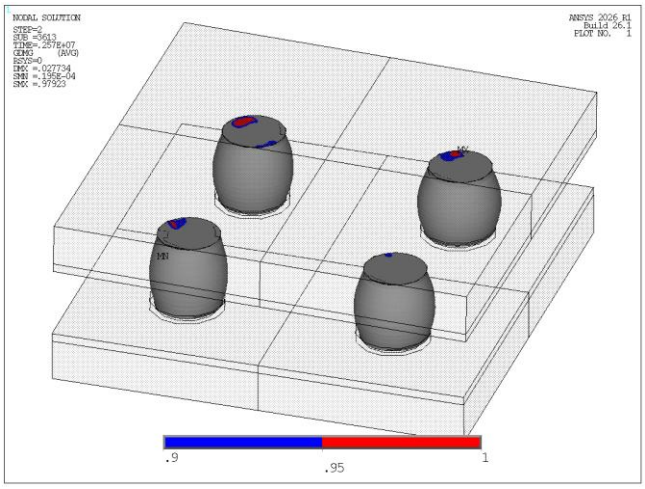
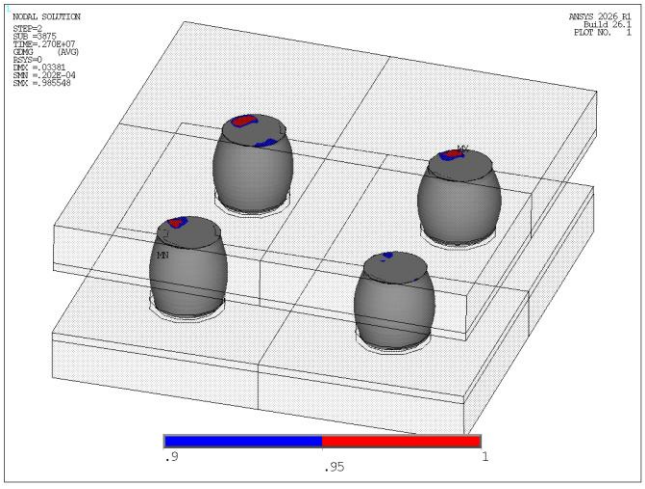


FIGURE 8: DAMAGE AT THE BOTTOM OF SOLDER-PAD INTERFACE AT 1000 CYCLES

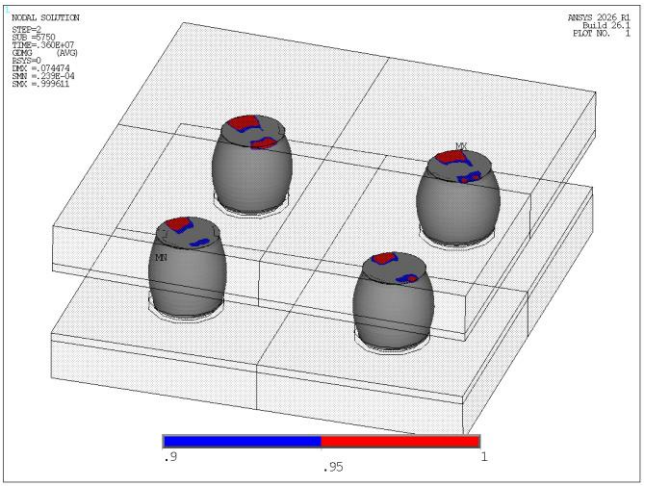
In this study, damage index larger than 0.95 is considered fully cracked. The detailed solder fatigue crack initiation and growth is displayed in Fig. 9. Again, mainly the top surfaces are shown as damages are concentrated and higher. As demonstrated in Fig. 9, the cracks start to initiate at the 3 solders near the interface at around 714 cycles. With further loading, crack also forms at the bottom right solder. The slower crack initiation at the bottom right solder is most likely due to the boundary constraint applied in the current model. Meanwhile, cracks also grow from outer interface to inside. It should be expected that crack would be fully connected from outside to inside at all solders with further loading. At 1000 cycles simulated, smaller cracks are also found at the bottom, as shown in Fig. 10. The simulated crack pattern agrees well with existing test finding in [2], [11], [12], where cracks are found to be near the interface between solder and copper pad. The exact accumulated cycles where crack initiates and fully propagation depend on the CDM model parameters selected in Table 1. Another interesting finding is if we compare the damage evolution for top right and bottom left solders, even though they have almost identical boundary conditions, the cycle when damage occurs is not the same. Similar observation is also found in [2] that solder shape has major influence on damage initiation. The obtained result clearly demonstrates the importance of accounting as reflowed solder shape in solder fatigue evaluation.



(a)



(b)



(c)

FIGURE 9: CRACK INITIATION AND PROPAGATION AT (A) 714 CYCLES, (B) 500 CYCLES, (C) 750 CYCLES, AND (D) 1000 CYCLES

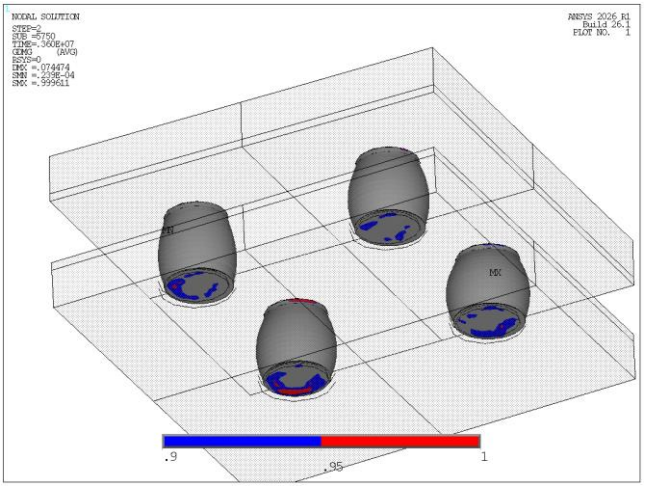


FIGURE 10: CRACK PATTERN AT THE BOTTOM OF SOLDER-PAD INTERFACE AT 1000 CYCLES

III. Conclusion

In this work, a multi-physics analysis workflow going from solder reflow to solder fatigue analysis is demonstrated. First, the as-reflowed solder shape is simulated by carrying out an ISPG solder reflow analysis on an example BGA. Then, a local region of interest with 4 solder balls is extracted from the center of the BGA where solder distortion is the highest. An in-house morphing algorithm is used to morph an all-hexahedral template solder mesh to the as-reflowed simulated geometry. This morphed mesh is then used in a thermal cycling analysis, where CDM is used to capture the impact of repeated thermal cycling and cycle jumping technique is employed to jump over cycles to reduce overall computational time over a large number of cycles. With this proposed workflow, the predicted as-reflowed solder shapes can be used directly without having to resolve to assume idealized shapes. This helps to capture the effects of distorted solder shapes in critical regions where solder distortion is severe to help uncover potential reliability weak spots in the BGA.

References

[1] Su, Sinan, Francy John Akkara, Ravinder Thaper, Atif Alkhazali, Mohammad Hamasha, and Sa'D. Hamasha. "A state-of-the-art review of fatigue life prediction models for solder joint." *Journal of Electronic Packaging* 141, no. 4 (2019): 040802.

[2] Liu, X. and Lu, G.Q., 2003. Effects of solder joint shape and height on thermal fatigue lifetime. IEEE Transactions on Components and Packaging Technologies, 26(2), pp.455-465.

[3] Pan, X., Wu, C. T., and Hu, W., 2020, Incompressible Smoothed Particle Galerkin Method for an Efficient Simulation of Surface Tension and Wall Adhesion Effects in the 3D Reflow Soldering Process, Proceedings of the 16th International LS-DYNA Conference.

[4] Pan, X., Wu, C. T., and Hu, W., 2020, A Semi-Implicit Stabilized Particle Galerkin Method for Incompressible Free Surface Flow Simulations, International Journal for Numerical Methods in Engineering, 121(17), pp. 3979–4002.

[5] Zou, J., Huang, M., Zhao, D., Chen, F., and Wang, D., 2023, Modeling the Contact Dispensing Process of Conductive Adhesives With Different Viscosities and Optimization of Droplet Deposition, Frontiers in Materials, 10, Article 1183747.

[6] Fang, M., Tang, C., Chen, Y., Li, J., Chen, Z., Wang, F., and Zhu, W., 2022, Thermo-Compression Bonding Process Characteristics and Shape Control of Cu-Pillar Microbump Joints by Optimizing Solder Melting, Journal of Materials Science: Materials in Electronics, 33, pp. 10471–10485.

[7] Amogh, S., Medikonda, S., Lyu, D., Sengupta, A., Mao, H., and M, S. K., 2024, Two-Scale Co-Simulation Approach for Drop-Test Simulation of Kovan PCB Board, Proceedings of the ASME International Mechanical Engineering Congress and Exposition, 88681, V010T12A034.

[8] Mao, H., Lyu, D., and Zheng, T., 2024, Advancing Solder Joint Modeling in PCBs: A Two-Scale Co-Simulation Approach for Shock and Vibration Analysis Using LS-DYNA, Proceedings of the 17th International LS-DYNA Conference.

[9] Yin, Bo, Imadeddin Zreid, Dong Zhao, Raasheduddin Ahmed, Guoyu Lin, and Michael Kaliske. "Thermomechanical fatigue life prediction of metallic materials by a gradient-enhanced viscoplastic damage approach." International Journal for Numerical Methods in Engineering 123, no. 9 (2022): 2042-2075.

[10] Sommitsch, Christof, Rainer Sievert, Thomas Wlanis, Burkhard Günther, and Volker Wieser. "Modelling of creep-fatigue in containers during aluminium and copper extrusion." Computational materials science 39, no. 1 (2007): 55-64.

[11] Zanella, S., 2018. Creep Fatigue Interaction in Solder Joint Alloys of Electronic Packages (Doctoral dissertation, Université Paris Saclay (COmUE)).

[12] Li, Lei, Xinyu Du, Jibing Chen, and Yiping Wu. "Thermal fatigue failure of micro-solder joints in electronic packaging devices: a review." *Materials* 17, no. 10 (2024): 2365.